

Paper

# Characterization of Cu(InGa)Se<sub>2</sub> (CIGS) Thin Films in Solar Cell Devices by Secondary Ion Mass Spectrometry

Weon Cheol Lim, Jihye Lee and Yeonhee Lee\*

Korea Institute of Science &amp; Technology, Seoul, Korea 136-791

\* yhlee@kist.re.kr

(Received: October 4, 2010; Accepted: January 18, 2011)

In this study, a quantitative analysis of Cu(InGa)Se<sub>2</sub> (CIGS) was performed using an electron probe microanalysis (EPMA) equipped with a wavelength dispersed spectroscopy (WDS), x-ray photoelectron spectroscopy (XPS), Auger electron spectroscopy (AES), and dynamic secondary ion mass spectrometry (dynamic SIMS). Reproducible quantitative analysis data were obtained for CIGS layers from a depth profile of SIMS and relative sensitivity factor (RSF) value calculated using the mole fraction of EPMA. In addition, to obtain a reproducible quantitative analysis for CIGS layers through SIMS depth profile, the experimental conditions were changed including the primary ion, beam energy, and beam current.

## 1. Introduction

Recently, as fossil fuels are becoming exhausted, many research groups are investigating the increasing efficiency of photovoltaics as an alternative source of energy.

Cu(InGa)Se<sub>2</sub> (CIGS) is one of the most useful materials for thin film photovoltaic devices due to its appropriate band gap and high absorption coefficient for solar radiation [1]. In CIGS film, the grading of the gallium (Ga) to indium (In) ratio affects the band gap grading and electrical fields that can either improve or degrade the performance of the solar cells, and are especially significant in the design of cells utilizing thin absorber layers [2, 3]. Another important factor is the growth of CIGS in the presence of sodium (Na), and the role of molybdenum (Mo) as a medium for Na transport [4-6].

As the importance of CIGS layers increases, quantitative analysis and characterizations of CIGS layers have been investigated [2-8]. In 2005, Yoon's research group attempted to obtain information on the chemical composition of CIGS nanoparticles using an energy dispersive spectroscopy (EDS) [7]. However, details of the composition profiles in few micrometer CIGS films were difficult to ascertain due to the electron beam and X-ray solid interactions that extended deep into the film depending on sample [3]. Herz *et al.* used simultaneous secondary ion

mass spectrometry/sputtered neutral mass spectrometry (SIMS/SNMS) to define the elemental concentration of the CIGS layers: they reported that the quantitative analysis through SNMS is possible for a minimum concentration of approximately 400 ppm [5]. Perkins *et al.* identified that the composition of CIGS thin films using EPMA equipped with wavelength dispersed spectroscopy (WDS), ICP-OES, and AES [2].

In 2007, Kim *et al.* also studied the procedure for determining the composition of binary alloy films, such as Fe-Ni, using the following equation [8]:

$$\begin{aligned} R_{Fe} &= I_{Fe}^s / C_{Fe}^s \\ R_{Ni} &= I_{Ni}^s / C_{Ni}^s \end{aligned} \quad (1)$$

where  $R_{Fe}$  is the relative sensitivity factor for an element Fe,  $I_{Fe}^s$  is the intensity of the standard material for a known composition of Fe,  $C_{Fe}^s$  is the certified composition for a known composition of Fe.

The SIMS composition of an unknown alloy film is calculated using the following equations:

$$X_{Fe}^{unk} = \frac{I_{Fe}^{unk}}{I_{Fe}^{unk} + I_{Ni}^{unk} / R}, R = \frac{R_{Ni}}{R_{Fe}}, \quad (2)$$

where  $X_{Fe}^{unk}$  is the composition of the unknown

element Fe.

In this work, the composition of the CIGS absorber layer was analyzed quantitatively because the CIGS composition is important in the performance of a device. And a quantitative analysis with repeatability is reported for CIGS layers and other experimental conditions affecting the SIMS depth profiling.

## 2. Experimental

The SIMS depth profiles were acquired in a Cameca IMS 4FE7 instrument. The primary ion was a Cs/O<sub>2</sub><sup>+</sup> ion beam. Secondary ions with positive polarity were detected as appropriate for the species being examined. The primary ion energies were 12.5 keV for the O<sub>2</sub><sup>+</sup> ion beam with the impact energies modified by the 4.5 keV potential of the sample. The depth profiles were obtained using a high primary beam current (100 nA) with the beam rastered over a 150 μm × 150 μm area. Non-impossible isotopes were used in order to minimize the mass interference.

The certified composition of the CIGS layers was defined by electron probe microanalysis (EMPA, JXA-8500F, JOEL, Japan) equipped with WDS. The AES spectra and depth profiles were taken on a Physical Electronics PHI 700 Scanning Auger Microscope. Depth profiling was performed using a 3 kV Ar<sup>+</sup> beam with a sputtering rate of 55.5 nm/min. The XPS measurement was performed on a Physical Electronics PHI-5800 using Mg Kα (1253.6 eV) radiation. The hemispherical energy analyzer was calibrated using the Ag and Au samples.

The CIGS samples were supplied by the Solar Cell Center in KIST. The depositions of the CIGS layer were evaporated and deposited on substrates in a vacuum chamber.

## 3. Results and Discussion

### 3.1. Comparative Atomic Concentration of EPMA, AES, and XPS for CIGS Samples

In general, the EPMA equipped with WDS is known to be an elemental quantitative instrument [2]. Also, the XPS and AES are quantitative analyzers with a several percent deviation for quantitative accuracy.

In order to compare the ability of the quantitative analysis of other surface instruments, such as XPS and AES, the atomic concentrations of WDS-EPMA were compared with the depth profile obtained through XPS and AES.

As shown in Table 1, most atomic concentrations of the elements have a difference of more than 10 percent. It was thought that the

use of pure elements as standards might cause large matrix-dependant errors.

As shown Figs. 1 and 2, the depth profiles of the AES and XPS were obtained as a coarser shaped depth profile.

Table 1. Atomic Concentration of CIGS Absorber.

Element	Instrumental Analysis		
	EPMA	AES	XPS
Cu	23.5 <sup>a</sup>	18.9 (-19.6) <sup>b</sup>	29.0 (+23.4)
In	19.2	29.5 (+53.6)	28.6 (+49.0)
Ga	7.9	8.8 (+11.4)	11.2 (+41.8)
Se	49.4	42.8 (-13.3)	31.2 (-36.8)

<sup>a</sup> is the atomic concentration. <sup>b</sup> is the deviation percentage compared with EPMA.

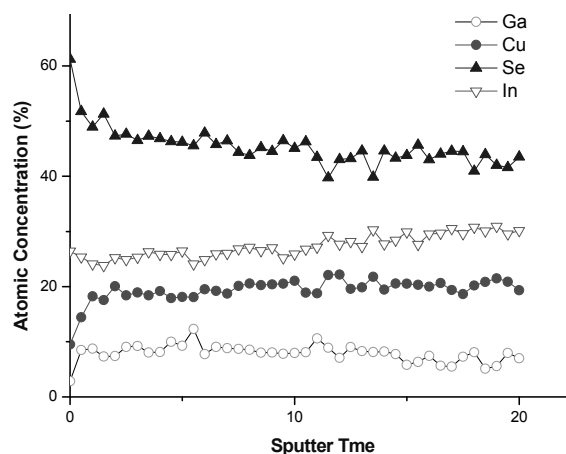


Fig. 1. AES depth profile of CIGS samples using a 3 kV Ar<sup>+</sup> beam.

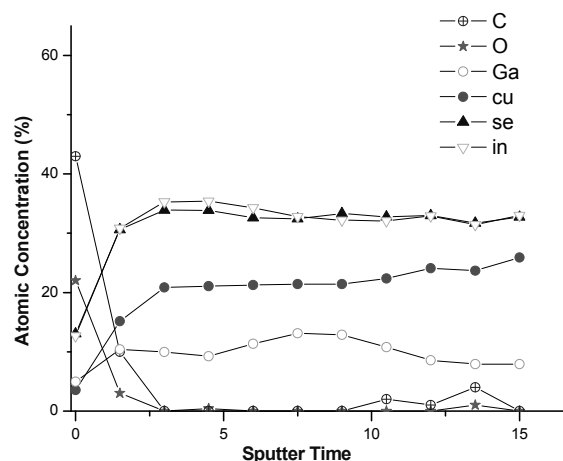


Fig. 2. XPS depth profile of CIGS samples using Mg Kα (1253.6 eV) radiation.

The composition of the CIGS absorber layer was analyzed using SIMS depth profiling

because it has an analysis advantage for diffusion of sodium and grading of gallium.[9,10] Moreover, SIMS has very low detection limits for trace elements while AES, XPS, and EPMA do not have sufficient sensitivity.

### 3.2. Quantitative Analysis of SIMS for CIGS Samples

Figure 3 shows the depth profile of the CIGS sample obtained using SIMS instrument. The Na and Ga grading was obtained as high intensities and is clearly distinguishable.

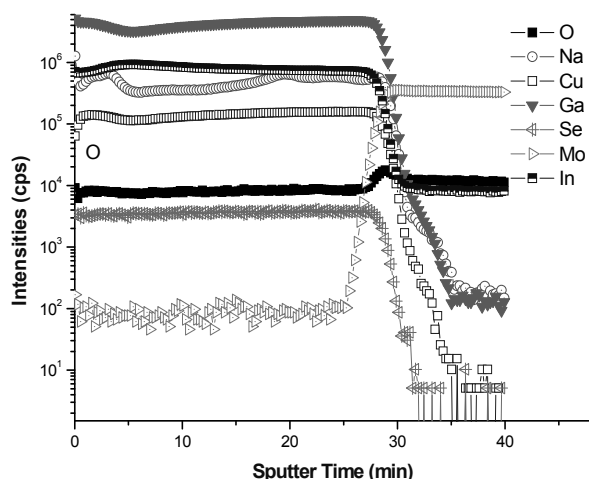


Fig. 3. SIMS depth profile of CIGS sample (K3701), the data were generated utilizing 8 keV O<sub>2</sub><sup>+</sup> ions with a primary ion beam current of 100 nA.

The WDS-EPMA results were used as a certified composition of the CIGS absorber layer. Then, the above equations were applied to the five elements in the CIGS layers: Cu, In, Ga, Se, and Na.

$$R_{Cu} = I_{Cu}^s / C_{Cu}^s, \quad (3)$$

The unknown composition of the CIGS absorber layers were calculated using the following equations:

$$X_{Cu}^{unk} = \frac{I_{Cu}^{unk}}{I_{Cu}^{unk} + \left( \frac{I_{In}^{unk}}{R^2} + \frac{I_{Ga}^{unk}}{R^3} + \frac{I_{Se}^{unk}}{R^4} \right)}, \quad (4)$$

$$\left( R^2 = \frac{R_{In}}{R_{Cu}}, R^3 = \frac{R_{Ga}}{R_{Cu}}, R^4 = \frac{R_{Se}}{R_{Cu}} \right)$$

Table 2 shows the differences in the atomic concentrations obtained by the EPMA and those calculated from the depth profiling undertaken by the dynamic SIMS.

Table 2. Atomic Concentration using Dynamic SIMS and WDS-EPMA. SIMS data was obtained using 8keV O<sub>2</sub><sup>+</sup>.

No. <sup>a</sup>	Cu	In	Ga	Se
K3701	24.0 <sup>b</sup>	14.4	12.2	49.4
K3702	26.0 (+8.1) <sup>c</sup>	15.8 (+9.9)	12.3 (+0.5)	47.8 (-2.9)
K3703	25.8 (+7.0)	16.0 (+10.5)	12.8 (+4.9)	45.3 (-7.7)
K3704	25.6 (+8.7)	15.6 (+5.5)	11.3 (-2.5)	47.4 (-4.2)
K5804	24.8 (+3.8)	15.4 (+2.9)	11.7 (-2.3)	48.1 (-0.4)

<sup>a</sup> is the different CIGS sample. <sup>b</sup> is the atomic concentration of EPMA. <sup>c</sup> is the deviation percentage compared with EPMA and dynamic SIMS.

To obtain an atomic concentration through dynamic SIMS, RSF for each element of CIGS was first calculated using the atomic concentration data of K3701 obtained through WDS-EPMA (equation 3). After obtaining the depth profiling of K3702, K3703, K3704, and K5804, the atomic concentrations were calculated using equation (4).

As shown in Table 2, the atomic concentrations of the elements have a difference of less than 10 percent, except for Na. Also, a repeatable atomic concentration was obtained within a 10 percent deviation for four CIGS samples. The atomic concentration of K3701 is similar to that of K5804, even if not made at the same time. In the future work, we plan to make quantitative analysis for trace element such as Na by using ICP-MS.

When a cesium ion beam is used, the intensity (or cps) of the CIGS samples was approximately one to two orders lower overall. Among the CIGS elements, the intensities of Cu were the lowest. However, the intensities of selenium maintained constantly when an oxygen beam was used.

When the cesium beam was used, there were difficulties in aligning the primary beam as it is a small, round beam and has a low depth resolution (Table 3). However, as the analysis time decreased, the intensity of selenium was similar to that of selenium when using an oxygen beam.

When lower impact energy was used, the intensity of the CIGS samples was approximately one order lower overall as shown in Table 4. Thus, the optimal impact energy for the CIGS analysis is above 8 keV. However, the depth resolution at 6 keV is similar to that at 8 keV.

Table 3. Effect of different primary ion beam.

Ion Beam	Ratio (Intensity)		Analysis Time (min)
	Ga (In + Ga)	Cu (In + Ga)	
Cs <sup>+</sup>	0.90 <sup>a</sup>	0.0017 <sup>a</sup>	30
O <sub>2</sub> <sup>+</sup>	0.89	0.010	35

<sup>a</sup> is positive secondary ion, M<sup>+</sup> was detected.

Table 4. Effect of Different Impact Energy. Data was obtained by using O<sub>2</sub><sup>+</sup>, 100nA.

Impact Energy <sup>a</sup>	Ratio (atomic conc.) <sup>b</sup>		Analysis Time (min)
	Ga (In + Ga)	Cu (In + Ga)	
6 keV	0.61	0.26	35
8 keV	0.44	0.89	35

<sup>a</sup> is the potential difference between the primary ion gun and sample stage. <sup>b</sup> is ratio compared atomic concentration of CIGS samples.

Table 5. Effect of Different Ion Current. Data was obtained using 8 keV O<sub>2</sub><sup>+</sup>.

Ion Current	Ratio (atomic conc.) <sup>a</sup>		Analysis Time (min)
	Ga (In + Ga)	Cu (In + Ga)	
50 nA	0.47	0.97	70
100 nA	0.44	0.89	33
150 nA	0.42	0.94	20

<sup>a</sup> is ratio compared atomic concentration of CIGS samples

When using various ion currents, the intensity of the CIGS samples and the depth resolution have little difference (Table 5). However, when the analysis time was decreased, the ratio of Ga to (In+Ga) decreases as the ion current increases.

#### 4. Conclusion

Various quantitative analyses of CIGS samples were performed using WDS-EPMA, XPS, AES, and SIMS. Repeatable quantitative analyses were obtained through the depth profiling of SIMS with a denser shaped grading than the AES and XPS. Also, a repeatable atomic

concentration was obtained within a 10 percent deviation for four CIGS samples. The results reported in this paper also indicated an optimized experimental condition, such as oxygen ion beam, above 8 keV of ion energy and above 100 nA of ion current.

#### 5. Acknowledgment

This research was supported financially by the Ministry of Education, Science and Technology of Korea. The authors would also like to thank Dr. Jung of the Solar Cell Center in KIST (Seoul, Korea) for supplying the CIGS samples.

#### 6. References

- [1] T. Wada, Y. Hashimoto, S. Nishiwaki, T. Satoh, S. Hayashi, T. Negami, H. Miyake, *Solar Energy Materials & Solar Cells*. **67**, 305 (2001).
- [2] C.L. Perkins, B. Egaas, I. Repins, *Appl. Surf. Sci.* **257**, 878 (2010).
- [3] M. Chandramohan, S. Velumani, T. Venkatachalam, *Mater. Sci. Eng. B*. **174**, 200 (2010).
- [4] A. Shah, P. Torres, R. Tsharner, N. Wyrsh, H. Keppner, *Science*, **285**, 692 (1999).
- [5] K. Hertz, A. Eicke, F. Kessler, R. Wachter, M. Powalla, *Thin Solid Films*, **431-2**, 392 (2003).
- [6] D.Niles, K. Ramanathan, F. Hasoon, R. Noufi, B.J. Tielsch, J.E. Fulghum, *J. Vac. Sci. Technol. A* **15**, 3044 (1997).
- [7] K. Kim, Y. Chun, K. Yoon, B. Park, *J. Mech. Sci. & Tech.* **19**, 2085 (2005).
- [8] K.J. Kim, D.W. Moon, C.J. Park, D. Simons, G. Gillen, H. Jin, H.J. Kang, *Surf. Interface Anal.* **39**, 665 (2007).
- [9] M. Bodegard, K. Granath, L. Stolt, A. Rockett *solar Energy Materials & Solar Cells*. **58**, 199 (1999).
- [10] G. Bilger, P.O. Grabitz, A. Strohm, *Appl. Surf. Sci.* **231**, 804 (2004).